Thermal Fatigue Test of an Annular Structure

Jeong-Ki Hwang*, Chang-Min Suh, Chae-Ho Kim
School of Mechanical Engineering, Kyungpook National University, 1370 Sankyuk-dong, Buk-gu, Daegu 702-701, Korea

A half-scaled large test model for the main components of the real annular structure was built and the thermal behaviors were experimented and obtained by thermal cyclic loads. The model design and the test conditions for the thermal loads were determined to take into consideration the thermal and mechanical loads acting on the real annular structure by finite element analyses. Temperature profiles and strains of the main components of the model were measured at an early stage of the test and periodically throughout the test in the given test conditions. After completion of the thermal cyclic tests, no evidence of crack initiation and propagation were identified by a dye penetration test. The measured strains at the critical parts were slightly increased proportionally with the increase in the number of the thermal cycles.

Key Words : Thermal Behavior, Fatigue Test, Thermal Loads, Thermal Cycle

1. Introduction

The operating conditions affect greatly structural design. Generally, the structural design is bound up with the service limits which define the stress levels in an elastic limit. Only a few structures are extended to their service limit beyond the elastic limit from an economical point of view when hostile operating conditions are encountered.

One of these structures is a permanent reactor cavity seal assembly, which is an annular structure welded to the seal ledge of a reactor vessel in nuclear power plants. This annular structure is a kind of dam to fill refueling water above the reactor vessel flange. The design of this annular structure is affected by the thermal expansion of the reactor vessel during power operation, earthquakes, or the static pressure of the refueling water during outage. Combination of the thermal expansion and/or the seismic loads requires a great effort to design the annular structure beyond the elastic limit.

This paper describes a structural model for the thermal test that was constructed and tested. The test condition for the thermal loads was derived from the simulation of the real annular structure by numerical methods when the thermal and seismic loads were applied. The tests were done on the basis of the thermal cycles which were defined in the plant design conditions. The structure was inspected by a dye penetration test after the thermal cyclic tests. During the thermal cyclic tests, the temperature profile of its flexure was measured.

Using the experimentally measured data, the finite element analysis model for the real annular structure was verified in order to reduce uncertainties during modeling processes.

* Corresponding Author,
E-mail : hjk@kopec.co.kr
TEL : +82-42-861-8201; **FAX** : +82-42-863-4862
School of Mechanical Engineering, Kyungpook National University, 1370 Sankyuk-dong, Buk-gu, Daegu 702-701, Korea. (Manuscript **Received** April 13, 2005; **Revised** December 7, 2005)

2. Experimental Test Model

2.1 Model description

Real annular structures such as the reactor cavity seal assembly in nuclear power plants are highly affected by temperature. This real annular

structure requires a careful approach to design (Hwang et al., 2004); thus, a structural model for the thermal cyclic tests was constructed and tested.

The diameter of the test model (C_d=2700 mm) was determined to half of the real structure, but the height (C_h=140 mm) was the same as the real one. The measured temperature profile of the test model during the test can be directly applied "as-measured" to the numerical model, because the temperature profile, which is greatly vulnerable to the modeling processes, is a major factor in the stress profile, and the initiation and the propagation of cracks, which are the local effects, are due to stresses of structures rather than a model similarity. A section of the test model is shown in Fig. 1.

The test model consists of a bottom plate, a flexure, a seal plate, and column supports. The bottom plate is a source of the thermal loads, partially contacted to the flexure and welded at its end (a in Fig. 1). The flexure is designed to absorb the thermal expansion of the bottom plate and the relative motion between the bottom plate and the seal plate. The seal plate is in partial contact with the flexure, and is welded at its end (b in Fig. 1). The column supports are evenly spaced along the seal plate and can withstand vertical loads, keeping the space between the seal plate and the bottom plate. These supports reduce the load acting on the flexure. The lower end of each column support stands on the bottom plate, and the top end is welded to the seal plate, which allows horizontal movement between the bottom plate and the seal plate.

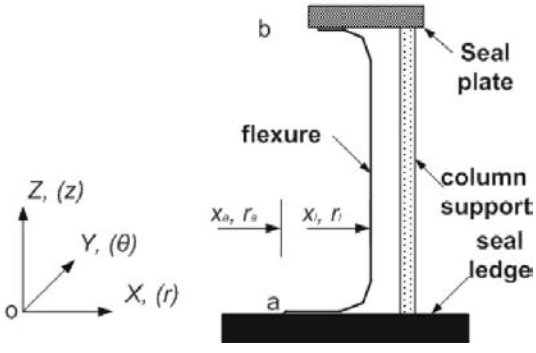

Fig. 1 Section of structural model

Table 1 Material specifications for test model

Components	Specifications	Thickness (mm)
Seal Ledge	A516 Gr 70	12
Flexure	A240 304	4
Seal Plate	A516 Gr 70	12

As the major object of the test is to identify the elastic and plastic behaviors of the flexure and its welding parts, the materials of the test model were thus selected with those of the real annular structure. The material specifications for the experimental test model are shown in Table 1.

2.2 Equilibrium equations

The annular structure is subjected to thermal loading, pressure, and relative displacements. The equilibrium equation of the structural model in Cartesian coordinates can be simply expressed as Equation (1).

$$[K]\{u\}=\{F_p\}+\{F_f\}+\{F_t\} \quad (1)$$

where $[K]$ is the stiffness matrix and $\{u\}$ is the displacement vector of the structural model. $\{F_p\}$, $\{F_f\}$ and $\{F_t\}$ are the static pressure load, the seismic displacement load, and the thermal load acting on the structural model, respectively.

2.3 Test conditions and analysis method

As the loading condition for the structural model is dependent upon the operating conditions of the real annular structure, the loadings for the structural model are combined on the basis of its operating conditions.

In the actual operating conditions of the real annular structure, the loading conditions are classified into two cases: one is combined with the thermal and the seismic displacement loads, and the other is combined with the static pressure and the seismic displacement loads. When the thermal and the displacement loads act on the real annular structure, the flexure is expected to have a relatively high stress level which is critical to the structural integrity. However, the flexure has relatively low stress level when the static pressure

is applied.

Consequently, the test was designed to focus on the application of the thermal loads and the seismic displacement loads. In order to determine the test condition, the real annular structure was simulated by FEM numerical methods (ANSYS, 2001) for the thermal and the displacement loads, and then the test structure was simulated with the same technique that is applied to the real annular structure except in the loading condition. During the analyses of the test structure, the thermal and the displacement loads were taken into consideration. However, the reactive load of the test structure against the seismic displacement loads was too high to handle; moreover, the test apparatus for the relative displacement were not readily available for use. Thus, only thermal tests for the structural model were performed. In order to include the seismic loading effect, the test temperature for the structural model was calculated to obtain the maximum stress level of the real annular structure with the input of the thermal and the seismic displacement loads. The test temperature is shown in Eq. (2). When a test temperature equivalent to the effect of the thermal and the displacement loads in the real annular structure was applied to the test model, the maximum stress had the same level along the circumference. However, when the thermal and the seismic displacement loads were applied to the real annular structure, the maximum stresses were shown locally.

$$T_f(r,\ \theta,\ 0) = 288℃ \tag{2}$$

For the thermal cyclic tests, 200 cycles which were defined on the design basis decided from operating conditions of the adjacent major structure were applied.

To better estimate the stress profile of the flexure, which is a main component of the real annular structure, the temperature profile of the flexure was measured during the thermal cyclic tests. Four test conditions for the temperature profile of the flexure are shown in Eqs. (3), and were established on the basis of the test temperature for the thermal cyclic test.

$$\begin{aligned} T_1(r,\ \theta,\ 0) &= 204℃ \\ T_2(r,\ \theta,\ 0) &= 232℃ \\ T_3(r,\ \theta,\ 0) &= 260℃ \\ T_4(r,\ \theta,\ 0) &= 288℃ \end{aligned} \tag{3}$$

3. Experimental Tests

3.1 Test apparatus

3.1.1 Heating and cooling apparatus

The electric heating method was applied to the test model, which was slow, steady, and safe, and which could be controlled easily and which provide a very homogeneous temperature. The electric heating plates (Fig. 2(a)) were specially ordered to fit the bottom plate of the test model and insulated to prevent heat loss during the test.

Figure 2 shows their setup for the test. The temperature controller of the heating plates was installed to control the temperature of the bottom plate. Cooling coils made of copper pipes were installed inside (Fig. 2(c)) and outside (Fig. 2(b)) the test model to reduce the cooling time.

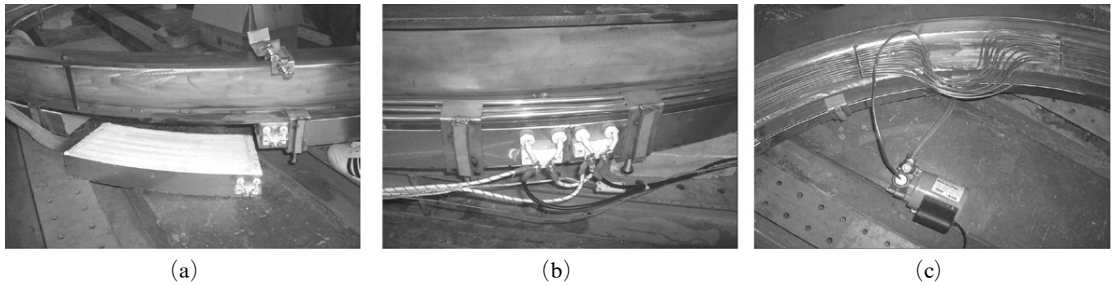

(a) (b) (c)

Fig. 2 Heating and cooling apparatus; (a) Electric heating plate (b) Setup of the plate and outside cooling coils (c) Setup of the plate and inside cooling coils

3.1.2 Method for strain and temperature measurements

The test temperature for the structural model was about 30% higher than the actual condition. Foil strain gauges (KFU-5-120-D16-11, gage length 5 mm) for elevated temperature strain at various temperatures were selected to measure high temperatures. Special treatments were done to cement the strain gauges with special adhesive, curing, and aging in series. The lead wires for the strain gauge were for high-temperature usage. The connections between the lead wires and the strain gauges were made with high-temperature solders considering the operating temperature. The strain measurements were taken with System 400 of the Measurement Group, which has muti-channels to get signals simultaneously. During the thermal cyclic test, the temperature of the flexure was measured to verify the thermal transfer analysis. The temperature measurements were done by thermocouples and a portable thermometer.

3.2 Thermal cyclic tests

3.2.1 Pre-test for strain gauge

A pre-test for the strain gauge were done on a specimen. The strain gauge was installed on the cantilever beam whose material was the same as that of the flexure and installed according to the procedures described briefly in Sec. 3.1.2.

Voltage from strain gauge was linearly proportional to the loads acting on the cantilever beam during the pre-test. The voltage was for the longitudinal direction of the cantilever beam, but the voltage for the wide direction was negligible. This test was done to justify the cementing procedures of the strain gauges.

3.2.2 Strain measurements and fatigue tests

Strain measurements were made at 6 locations : three of them were classified as major locations, while the others were as additional ones. The three major locations had 9 measuring points each, and the three additional locations had 2 measuring points each. The measuring locations and points are shown in Fig. 4. Table 2 shows the terminal classifications and numbers of the strain gauges. In the terminal classification, the first numbers are for circumferential locations, the second capitals are for the direction (H : horizontal direction along the circumference, V : stands for vertical directions along the section of the flexure), the third numbers are for positions, and the fourth capitals stand for inside (I) or outside (O). For example, 1H2I stands for Location 1, Horizontal direction, Position 2 and Inside of the flexure. The measuring positions of the strain gauges were determined by analysis of the structural model.

The thermal cyclic tests for the structural model were performed for 200 cycles which were defined in the design bases of adjacent major component

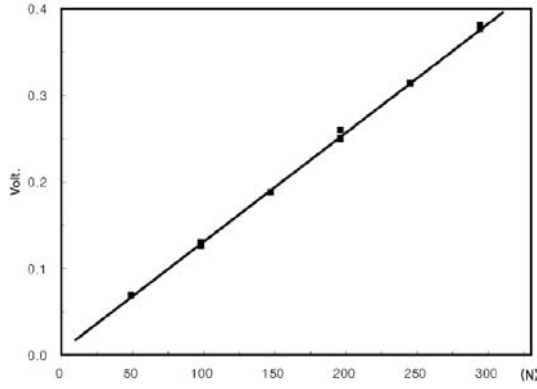

Fig. 3 Voltage from strain gauge depending on thermal loads

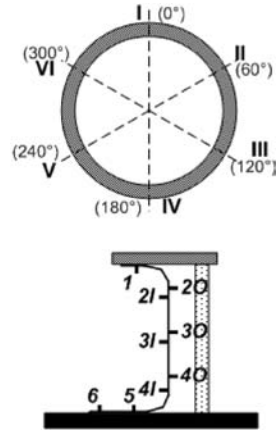

Fig. 4 Nomenclature of measuring positions for elevated temperature strains

Table 2 Nomenclature and terminal classification

Circumferential locations	Sectional positions						No. of terminals
	1	2	3	4	5	6	
I	1H1I, 1V1I	1H2I, 1V2I 1H2O, 1V2O	1H3I, 1V3I 1H3O, 1V3O	1H4I, 1V4I 1H4O, 1V4O	1H5I, 1V5I	1H6I, 1V6I	18
III	3H1I, 3V1I	3H2I, 3V2I 3H2O, 3V2O	3H3I, 3V3I 3H3O, 3V3O	3H4I, 3V4I 3H4O, 3V4O	3H5I, 3V5I	3H6I, 3V6I	18
V	5H1I, 5V1I	5H2I, 5V2I 5H2O, 5V2O	5H3I, 5V3I 5H3O, 5V3O	5H4I, 5V4I 5H4O, 5V4O	5H5I, 5V5I	5H6I, 5V6I	18
II, IV, VI	2H4I, 2H4O 4H4I, 4H4O, 6H4I, 6H4O, 2V4I, 2V4O, 4V4O, 4V4O, 6V4I, 6V4O						12

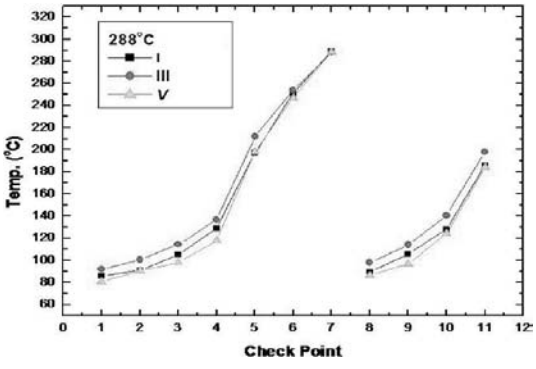

Fig. 5 Variation of temperatures at 288℃ on location I, III and V

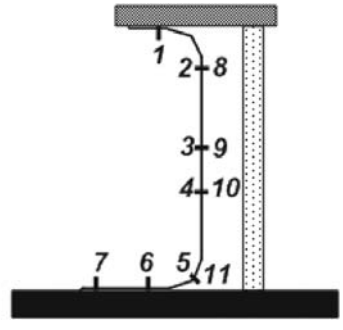

Fig. 6 Positions for temperature measurement

(Korea Electric Company). One thermal cycle of Eq. (3) involved heating the seal plate of the test model from room temperature up to 288℃, and then cooling it from 288℃ down to room temperature.

When the temperature of the bottom plate reached 288℃, 10 minutes were allowed to stabilize of the structure's temperature. The strain data were measured at intervals of 10 minutes, but all the cycles were not recorded.

The measured strain data at the 165th cycle and at location 4 (IV in Fig. 4) are shown in Fig. 5. The acquisition time of strain data for one thermal cycle lasted more than 4 hours ; thus, four fans were operated when cooling the structural model.

3.2.3 Temperature measurements

During the thermal cyclic test, the temperature profile of the flexure was measured and recorded. The temperature was measured at the locations I, III, and V around the circumference, as shown in Fig. 4, and at eleven positions along the section of the flexure, as in Fig. 6. The temperature for the flexure was measured when the temperature of the bottom plate was at 204℃, 232℃, 260℃, and 288℃, respectively.

The measured data were for the verification of the thermal analysis of the real annular structure. Fig. 5 shows an example of these data which were obtained at the situation of natural convection in case of 288℃.

4. Discussion

4.1 Strain measurements

As shown in Fig. 7, the horizontal strains are higher value than the vertical ones at the vertical section of the flexure, and the measured data have relatively small values in comparison with those of the analyses, which indicate that the strains have some fluctuations due to the thermal beha-

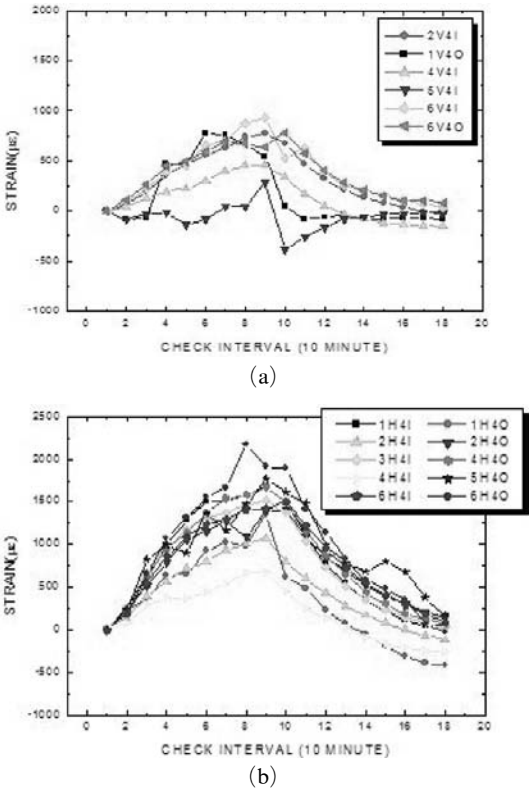

Fig. 7 Measured strains on location 4 and at the 165th cycles in (a) Vertical direction and (b) Horizontal direction

vior for temperature profile around the bent parts of the flexure.

The measured data at the same locations on every position have relatively large deviations, but show the same trends. These deviations seem to be the real data because a half-scaled model is closer to the real annular structure than an experimental scale in the laboratory, and the manufacturing tolerance of the test structure was applied to the real annular structure.

The strains at position 4Is and 4Os had the maximum strain values among those measured, and some of them exceed the elastic limit by 0.2%. However, the average strains did not exceed the elastic limit. Strains measured outside (O) of the flexure had larger values than those inside (I) because of the bending effects of the thermal expansion. The average strains at location 4 are slightly increased proportionally with the increase

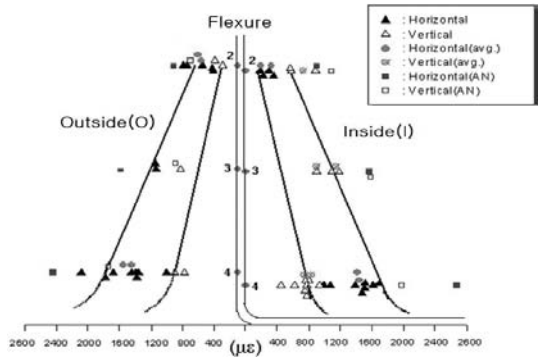

Fig. 8 Comparison of strain variation with the measurement data and finite element analysis

in the number of thermal cycles. The strain increments seem to be an accumulated plastic deformation of the flexure from a macroscopic point of view, because the strains at all other locations except for location 4 are slightly increased or decreased proportionally to the number of thermal cycles. Thus, the low bent part of the flexure, which has severe bending motion, has a thermal plastic deformation. The strains of the flexure which were the measured data and the finite element analysis results, are compared in Fig. 8. The measured data are much less than those of analyses; thus, the finite element analysis results were conservative from the design point of view.

4.2 Temperature measurements

Figure 9 shows an example of the variation of temperature and position. The measured temperature profiles are well trended to each other; therefore, the measured data can be regarded as authentic.

Thermal analyses for the structural model were carried out on the basis of the measured temperature. Using the equation for the heat transfer coefficient (Holman, 1986) and conduction elements (ANSYS, 2001), the thermal analysis model was verified by comparison between the measured and analysis data, as shown in Fig. 10. The measured temperature could be utilized to prove the reliability of the thermal analysis model because the temperature profile of the flexure is critical to the stresses of the structure.

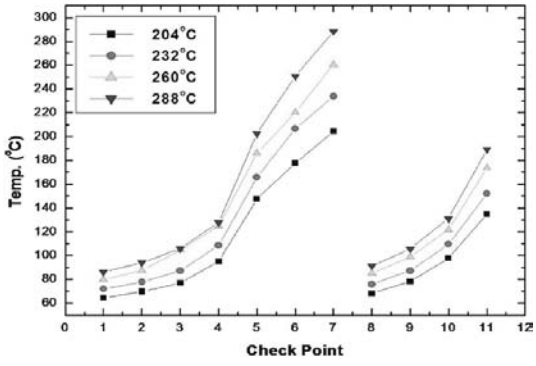

Fig. 9 Variation of average temperature according to the measured positions and temperatures

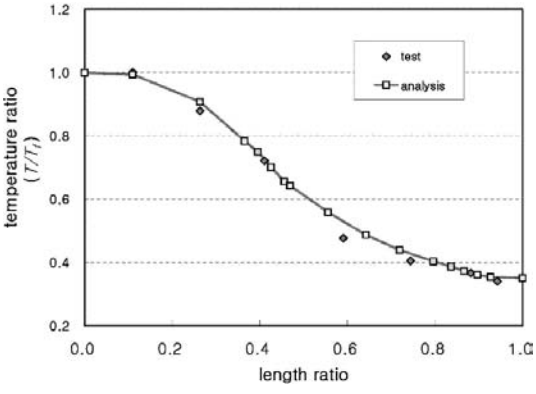

Fig. 10 Comparison of temperature ratio with the experimental data and analysis one

4.3 Dye penetration test

By a dye penetration test after 200 cycles of the thermal loads, the surfaces (Suh et al., 1990; 1992) of the main components were inspected. The inspection was done 20 minutes after spraying the developing solution. There were no indications or symptoms that the cracks had been initiated or propagated. Only a grinding surface on the weld got spotted with the dye locally.

5. Conclusions

A half-scaled large test model for a permanent reactor cavity assembly was tested to verify its structural integrity. During thermal cyclic loads, the temperature and strain profiles of the flexure were measured and recorded. After completion of the thermal cyclic loads, a dye penetration test was performed, and there was no evidence for failure of the major components. Some strains at the critical part of the flexure slightly increased proportionally with the increase in the number of thermal cycles. Finite element analysis results for the test model were conservative in comparison with those of the measured one. Using the measured data, finite element analysis models for the real annular structure were verified in order to reduce uncertainties during modeling processes.

References

ANSYS, 2001, "User's Manual," ANSYS Inc.

Holman, J. P., 1986, Heat Transfer, Chapter 6, McGraw-Hill, New York.

Hwang, J. K., Kim, I. Y. and Choi, T. S., 2004, "Development of Permanent Reactor Cavity Seal Assembly for Operating Nuclear Power Plants," Proceedings of the 2004 International Congress on Advances in Nuclear Power Plants, pp. 800~804, ICAPP'04, Pittsburgh, USA.

Korea Electric Company, Final Safety Analysis Report — Kori Nuclear Power Plant Unit No. 2, Chapter 3.

Korea Electric Company, Preliminary Safety Analysis Report — Korea Nuclear Units 7 & 8, Chapter 3.

Suh, C. M., Lee, J. J. and Kang, Y. G., 1990, "Fatigue Microcracks in Type 304 Stainless Steel at Elevated Temperature," Fatigue Fract. Engng. Mater. Struct., Vol. 13-5 : pp. 487~496.

Suh, C. M., Lee, J. J., Kang, Y. G., Ahn, H. J. and Woo, B. C., 1992, "A Simulation of the Fatigue Crack Process in Type 304 Stainless Steel at 538 C," Fatigue Fract. Engng. Mater. Struct., Vol. 15-7, pp. 671~684.